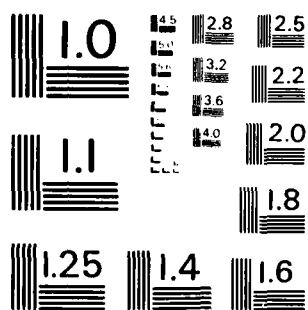END

DATE
FILMED

DTIC

MICROCOPY RESOLUTION TEST CHART

NATIONAL BUREAU OF STANDARDS - 1963 - A

NSWC MP 83-116

MICROSTRUCTURAL ORIGINS OF HOT SPOTS IN RDX EXPLOSIVE AND SEVERAL REFERENCE INERT MATERIALS

ANNUAL PROGRESS REPORT NO. 1 FOR PERIOD 30 DEC 1981 TO 30 SEP 1982
WORK REQUEST NUMBERS N00014-82-WR-20129 (WORK UNIT NUMBER NR659-797)
AND N00014-82-K-0263 (WORK UNIT NUMBER NR659-798)

W. L. ELBAN, C. S. COFFEY, AND R. W. ARMSTRONG*
RESEARCH AND TECHNOLOGY DEPARTMENT

AND

K. - C. YOO* AND R. G. ROSEMEIER*
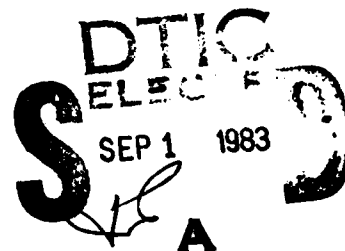
* MECHANICAL ENGINEERING DEPARTMENT
UNIVERSITY OF MARYLAND, COLLEGE PARK

MARCH 1983

DTIC
ELECTE
SEP 1 1983
S
A

DTIC FILE COPY

NAVAL SURFACE WEAPONS CENTER

Dahlgren, Virginia 22448 ● Silver Spring, Maryland 20910

83 08 31 013

SECURITY CLASSIFICATION OF THIS PAGE (When Data Entered)

REPORT DOCUMENTATION PAGE		READ INSTRUCTIONS BEFORE COMPLETING FORM
1. REPORT NUMBER NSWC MP 83-116	2. GOVT ACCESSION NO. AD-A132056	3. RECIPIENT'S CATALOG NUMBER
4. TITLE (and Subtitle) MICROSTRUCTURAL ORIGINS OF HOT SPOTS IN RDX EXPLOSIVE AND SEVERAL REFERENCE INERT MATERIALS		5. TYPE OF REPORT & PERIOD COVERED Progress Report FY82
		6. PERFORMING ORG. REPORT NUMBER
7. AUTHOR(s) W. L. Elban, C. S. Coffey, R. W. Armstrong, K. C. Yoo, R. G. Rosemeier		8. CONTRACT OR GRANT NUMBER(s) N00014-82-WR-20129 N00014-82-K-0263
9. PERFORMING ORGANIZATION NAME AND ADDRESS Naval Surface Weapons Center (Code R13) White Oak, Silver Spring, MD 20910 and University of Maryland, College Park, MD 20742		10. PROGRAM ELEMENT, PROJECT, TASK AREA & WORK UNIT NUMBERS 61153N; RR024-02-OD; 0; 659-797(798)
11. CONTROLLING OFFICE NAME AND ADDRESS Office of Naval Research 800 N. Quincy Street Arlington, VA 22217		12. REPORT DATE March 1983
		13. NUMBER OF PAGES 42
14. MONITORING AGENCY NAME & ADDRESS(if different from Controlling Office)		15. SECURITY CLASS. (of this report) UNCLASSIFIED
		15a. DECLASSIFICATION/DOWNGRADING SCHEDULE

16. DISTRIBUTION STATEMENT (of this Report)

Approved for public release; distribution unlimited.

17. DISTRIBUTION STATEMENT (of the abstract entered in Block 20, if different from Report)

18. SUPPLEMENTARY NOTES

Reproduction in whole or part is permitted for any purpose of the United States Government.

19. KEY WORDS (Continue on reverse side if necessary and identify by block number)

Hot Spot	Berg-Barrett X-Ray Topography	Drop-Weight Impact Testing
RDX Explosive	Synchrotron X-Ray Topography	
MgO	Hardness	
NaCl	Microhardness	

20. ABSTRACT (Continue on reverse side if necessary and identify by block number)

Hardness testing is being used to locally deform RDX explosive and several selected reference inert crystals in a controlled manner in order to investigate the microstructural origins of hot spots. The plastic deformation in RDX was found to be very inhomogeneous. The strain fields around Knoop hardness impressions in a reasonably perfect laboratory-grown crystal were studied using surface reflection Berg-Barrett

DD FORM 1473 1 JAN 73   EDITION OF 1 NOV 65 IS OBSOLETE
S/N 0102-LF-014-6601

20. (Cont.)

topography. Highly localized strain fields were observed, and a considerable anisotropy in Knoop hardness number was measured. A substantial variation in Vickers hardness numbers was obtained for several Holsten production-grade Class D RDX crystals. This is indicative of this material's inhomogeneous internal structure; perhaps most notable is the presence of numerous pores observed by microscopic examination.

Spherical ball hardness experiments at various applied loads were performed on a single crystal of MgO. Examination of the strain fields surrounding the resultant impressions by surface reflection Berg-Barrett topography revealed that, for increasing applied loads, the size of the strain fields was controlled by cracking. The strain fields around hardness indentations placed in a single crystal of NaCl were also investigated, in collaboration with other researchers, by synchrotron X-Ray topography.
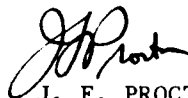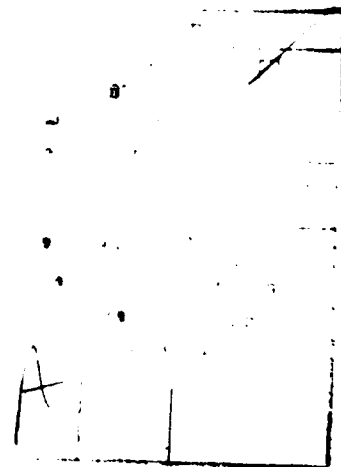
S N 0102- LF- 014- 6601

FOREWORD

This work was sponsored by the Office of Naval Research under work request numbers N00014-82-WR-20129 and N00014-82-K-0263 as a cooperative effort between NSWC, White Oak, and the University of Maryland, College Park. The results and conclusions presented in this report concerning the microstructural characterization of deformed RDX explosive and selected reference inert (MgO and NaCl) crystals should be of interest to those studying plastic deformation and fracture in these materials. In particular, this work provides insight into their ability to locally concentrate energy as a result of being plastically deformed in a controlled manner. A listing of references appears on several pages after the body of the report.

Dr. J. W. Cleland of the Solid State Division of the Oak Ridge National Laboratory supplied the MgO crystal.

Approved by:

J. F. PROCTOR, Head
Energetic Materials Division

CONTENTS

ILLUSTRATIONS

INTRODUCTION

It is well known that for initiation to occur in a solid explosive under impact conditions, the energy transferred must be concentrated into small volumes of the explosive. The most widely-held view explaining this phenomenon involves the formation of "hot spots" as a result of the explosive experiencing a mechanical stimulus. Heat is generated within a fixed volume at a sufficient rate to cause the temperature to rise very rapidly, the kinetics being limited by the thermal conductivity to the surrounding medium. A number of mechanisms, including adiabatic compression of small entrapped bubbles of gas, friction (between explosive particles and between explosive and impact tools), shear deformation, and fracture, have been envisioned as leading to hot spot formation in crystalline explosives.[1,2]

The role that localized behavior plays in the impact initiation of explosives has been investigated by striking single crystal targets (explosive) with tiny spherical particles (inert).[3] Initiation resulted when critical conditions for particle size and velocity were exceeded. A nice feature of this experiment is the ability to examine and characterize the deformation that resulted when the impact conditions were slightly below the critical conditions necessary for initiation. Typically, the impact sites were smooth plastic indentations and few fractures were found. It was observed further that the deformation was highly localized in narrow bands of material, which were proposed to form by adiabatic shear. It was also suggested that the mechanism responsible for initiation was the production of high local temperatures as a result of the adiabatic shear deformation.

It is consistent with dislocation theory concepts that deformation in crystalline solids occurs by localized deformation twinning or along slip planes that form into local shear bands. Similar inhomogeneous deformation behavior occurs for partially crystalline or even amorphous material. The bulk of the material, which is not in the shear bands, remains undeformed. A dislocation description of localized shear deformation that occurs within a model slip band indicates that appreciable heating can occur where a pile-up is released suddenly in an avalanche mode.[4] To date, no temperature measurements have verified directly that shear bands are hot spot sites. However, this may be inferred from related experiments. It has been reported that the temperature at the tip of a propagating crack, where highly localized plastic deformation is known to be occurring, is in excess of 500°K for polymethylmethacrylate,[5] in excess of 3200°K for glass, and about 4700°K for quartz.[6]

In an effort to determine the temperatures generated when various energetic materials are impact loaded, a limited study[7] was performed on HMX (cyclotetramethylenetetranitramine) explosive using a heat sensitive film as a detector. Substantial deformation and fracture accompanied by discoloration of the film (calibrated as indicating temperatures greater than 220°C for the impact loading conditions of this work) occurred when a single crystal of HMX (approximately 900 µm) was impacted from 5 cm, but no reaction resulted. At a 10 cm drop height, enough heating took place to cause an ignition reaction which died out. The reaction occurred in the most heavily deformed region of the crystal. Very little heating resulted when a 30 mg pile of Class A HMX was impacted at a 10 cm drop height.

For these experiments the energy imparted to the explosive sample was insufficient to heat the entire sample to its ignition temperature. However, it is clear that large temperature rises can result when explosive crystals, such as HMX, are deformed on impact, and that this heat production must be localized, i.e., hot spots are formed. It is also clear that the heat generation is related to the deformation that takes place in the explosive crystal. The mechanics of deformation in explosive crystals remains to be determined, along with answering how the actual resultant crystal defect structure relates to hot spot formation.

Individual explosive crystals themselves are not typically of convenient size for many of the well-defined deformation experiments normally performed on other types of materials. Microhardness testing[8] provides a controlled way of locally deforming these crystals offering information concerning the active slip systems and the degree of plastic anisotropy. Normally, two types of indenters are employed: Vickers or diamond pyramid and Knoop. The Vickers indenter has an apex angle of 136°. The Knoop indenter is more blunt than the Vickers; a diagonal indentation results that is seven times longer in one direction than in the other. It also yields a more shallow indentation which makes Knoop testing very suitable for studying brittle materials such as explosive crystals. It is the Knoop test that is used to investigate[9] plastic anisotropy.

In previous work,[10,11] the degree of localized plastic deformation was determined for RDX (cyclotrimethylenetrinitramine) explosive crystals grown at NSWC. Microhardness indentations were placed on various growth facets of several large (a few mm) size crystals that were grown from solution in acetone by evaporation at room temperature. Both Knoop and Vickers indentations were made at a 50g load with the orientation of the long axis of the Knoop indenter being allowed to vary with respect to specific surface directions in the growth facets. For the combined measurements on all of the growth facets, a considerable variation in Knoop hardness number was obtained (values ranged from 17 to 71 kgf/mm^2), suggesting a limited number of operative slip systems. An etch pit technique[12] was used to determine the extent of the plastic zone or strain field associated with each indentation. Highly localized etch pit arrays centered on the indentations were observed with the surface area of the plastic zones being only about 11 times greater than the projected area of the indentations. In a preliminary comparative study of production-grade (Holsten) Class D RDX crystals (usually 1-2 mm), Knoop hardness numbers compared well with values obtained for laboratory-grown crystals.
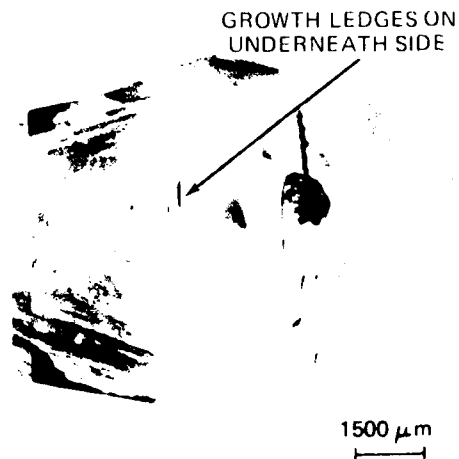
2

The objective of this current work is to further elucidate the fundamental microstructural reasons for hot spots being generated during the deformation of crystalline energetic and inert materials. The deformation behavior of RDX, the most common ingredient in Navy explosives, is being investigated at NSWC. Emphasis is being given to comparing various laboratory-grown crystals having different degrees of microstructural perfection and production-grade crystals. This work is closely allied with a companion research effort on selected model inert crystals at the University of Maryland, College Park.

CHARACTERIZATION AND DEFORMATION OF RDX

A large laboratory RDX crystal (Figure 1(a)) grown by Dr. R. Y. Yee (Naval Weapons Center, China Lake, CA) was studied using Laue and Berg-Barrett X-ray diffraction techniques. This crystal was grown by slow evaporation from acetone solution using a seed; the starting material was recrystallized Holsten production-grade crystals chemically manufactured[13] by the nitration of hexamethylenetetramine. The morphology of this crystal, as determined from a zone analysis of its Laue back-reflection photograph, was found to be the same as for the non-standard morphology of some of the laboratory RDX crystals grown[10,11] previously at NSWC. Various growth surfaces and crystal directions are specified in Figure 1(b). The degree of microstructural perfection of this crystal is significantly improved compared to crystals grown at NSWC, as evidenced by the absence of optical dispersion. In addition, most of the diffraction spots on the Laue photograph were sharp. However, some streaking for a few spots was observed. The lines visible in Figure 1(a) are associated with growth ledges on the bottom of the crystal. The overall crystal thickness was ~ 5 mm.

Preparatory to studying systematically the deformation properties of Dr. Yee's crystal, considerable effort was devoted to its microstructural characterization by surface reflection Berg-Barrett topography. This technique (Figure 2(a)) involves recording the structure in an individual Laue back-reflection spot under appropriate geometrical conditions on a fine-grained nuclear emulsion plate or film.[14] Local variations in diffracted intensity (Figure 2(b)) can be associated directly with internal strains in the crystal surface layer from which the X-ray beam is diffracted (i.e., the extinction depth).[15] The use of Berg-Barrett topography for examining the microstructure of crystalline materials has been discussed in detail.[14,16,17]

Prior to obtaining the first topograph, two Knoop indentations (50 g load) were placed (Figure 3(a)) in the top portion of the $(\bar{2}10)$ growth surface to serve as recognizable features that would offer some variation in contrast in the topograph. The long axis of the indenter was aligned parallel to $[00\bar{1}]$. For one indentation, the $(\bar{2}10)$ surface fully supported the indenter. For the other indentation, the indenter was only partially supported by the $(\bar{2}10)$ surface, and a large crack resulted. No particular care was taken to insure orthogonality between the applied force axis of the indenter and the $(\bar{2}10)$ surface. The strain fields of these two indentations are readily apparent in the topograph for the $(\bar{7}2\bar{1})$ reflection appearing in Figure 3(b). The enhanced

3

GROWTH LEDGES ON
UNDERNEATH SIDE

1500 μm

(a) LIGHT (ZEISS TESSOVAR) PHOTOGRAPH

1500 μm
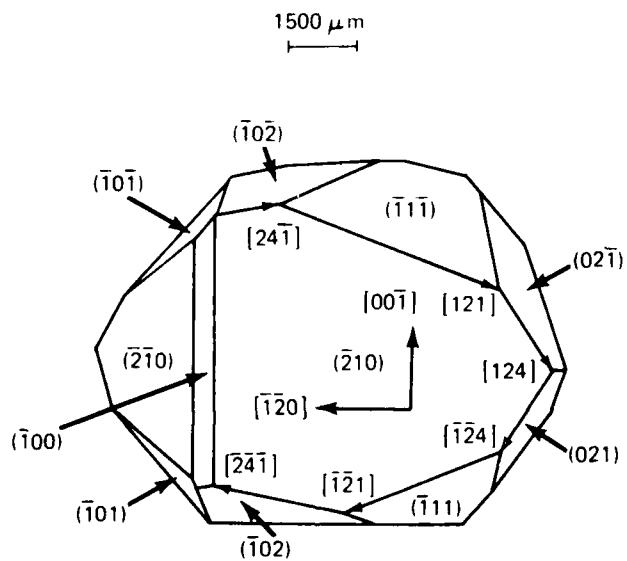
(b) SCHEMATIC IDENTIFYING EXPOSED GROWTH SURFACES AND DIRECTIONS

FIGURE 1.   LABORATORY–GROWN CRYSTAL

4
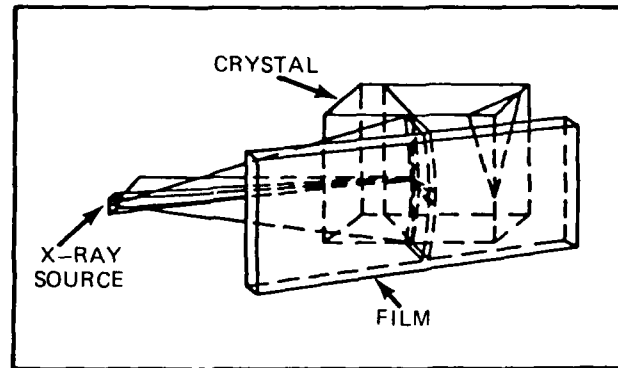
(a) EXPERIMENTAL CONFIGURATION
(AFTER REFERENCE 14)
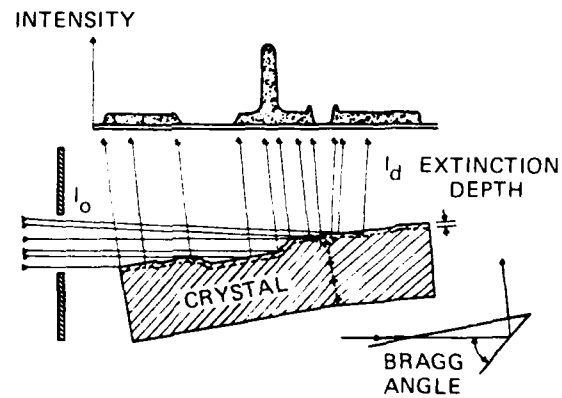
(b) CRYSTAL IMPERFECTION CONTRAST EFFECTS
(AFTER REFERENCE 15)

FIGURE 2. SCHEMATIC OF SURFACE REFLECTION BERG-BARRETT TOPOGRAPHY TECHNIQUE
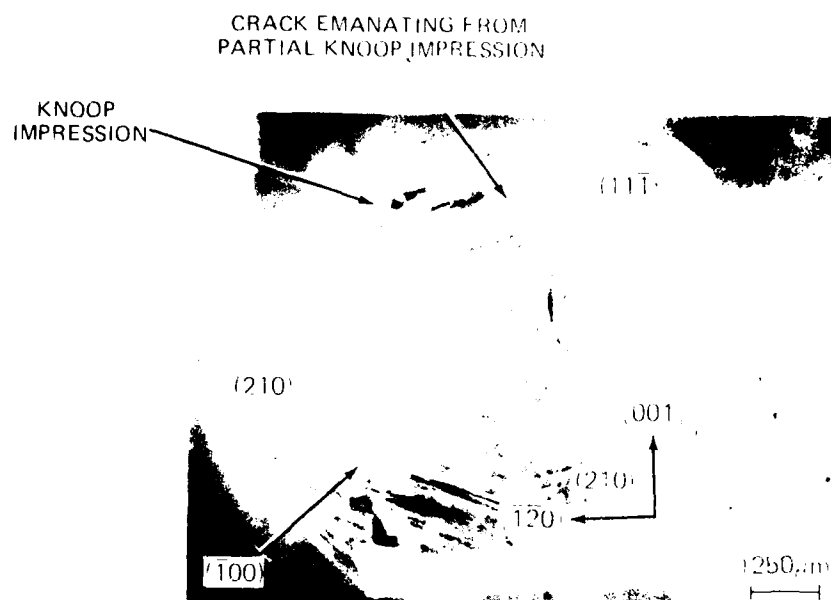
CRACK EMANATING FROM
PARTIAL KNOOP IMPRESSION

KNOOP
IMPRESSION

(111)

(210)

001

(210)

120

100

1250 μm

(a) LIGHT (ZEISS TESSOVAR) PHOTOGRAPH

[001]

q [721]

1500 μm
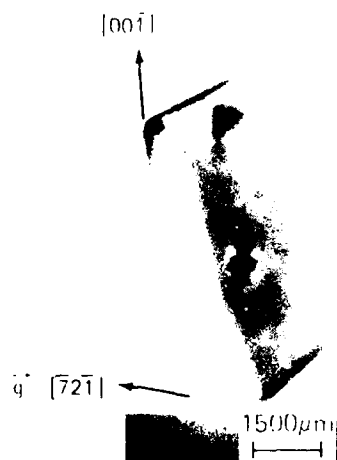
(b) X RAY SURFACE REFLECTION TOPOGRAPH

CuKα RADIATION AT 14 kV AND 20mA FOR
3 h ON ILFORD L4 50 μm NUCLEAR PLATE

FIGURE 3.   LABORATORY–GROWN RDX CRYSTAL AND BERG-BARRETT TOPOGRAPH
((721) REFLECTION)

diffracted intensity occurs because of the cumulative residual dislocation strain fields that resulted from accommodating the indenter. Also visible in this topograph is a large growth strain center associated with grown-in dislocations emanating from the seed crystal to the $(\overline{2}10)$ growth surface.

A topograph having significantly improved resolution appears in Figure 4(a) for the $(\overline{6}3\overline{2})$ reflection. This improvement was primarily the result of being able to reduce the film-to-specimen distance from 10 to 4 mm without overlapping images becoming a problem. A stereographic description for the Berg-Barrett X-ray topography alignment used in obtaining both a $(\overline{7}2\overline{1})$ and a $(\overline{6}3\overline{2})$ reflection image is given in Figure 5.

Extensive Knoop hardness testing (50 g load) was performed on the $(\overline{2}10)$ growth surface in regions not influenced by the large growth strain center to assess systematically the degree of plastic anisotropy. No effort had been made in previous hardness experiments[10,11] on RDX to select regions of the crystal that were reasonably strain-free. Now, care was taken to maintain orthogonality between the applied force axis of the indenter and the $(\overline{2}10)$ growth surface by leveling the crystal each time prior to indenting it. The hardness anisotropy for this growth surface is shown in Figure 6, with maximum hardness near the [124]. Significant cracking and corresponding lower hardness values occurred when the indenter was aligned along the $[\overline{2}4\overline{1}]$. This suggests that the amount of plastic deformation under the indenter for this particular arrangement is extremely limited. Consistent with hardness anisotropy measurements on NSWC laboratory-grown crystals,[10,11] a considerble anisotropy in Knoop hardness number was obtained for this more perfect laboratory-grown RDX crystal. This anisotropy indicates that a limited number of slip systems are operative and that cross slip (dislocation maneuverability) is very difficult.[18]

The strain fields of the indentations are delineated in the $(\overline{6}3\overline{2})$ reflection image in Figure 4(b). The absence of any diffracted intensity at the actual indentation sites is the result of the severe strains there. Immediately adjacent to these zero diffracted intensity zones are tiny black regions of enhanced diffracted intensity. The observed highly localized strain fields confirm a previous dislocation etch pit study[10] on an indented NSWC crystal. This result and the large degree of plastic anisotropy indicate that plastic deformation is very inhomogeneous in RDX, even in reasonably perfect crystals.

Vickers hardness experiments (50 and 100 g load) were performed on the (001) growth face of a number of Holsten production-grade Class D RDX crystals, typically 1-2 mm in size (Figure 7(a)). Measurements at 100 g load allowed better resolution of the crystallographically-determined crack traces (Figure 7(b)) that emerged in the (001) surface. Vickers hardness numbers of 30 and 50 kgf/mm^2 were obtained for two crystals at 100 g load with one pyramid diagonal being roughly parallel (within 10-11½°) to [110]. Aligning the pyramid diagonal considerably off [110] yielded badly distorted impressions that were not suitable for hardness measurements. However, varying the indenter diagonal alignment did not substantively alter the crystallographic alignment of the cracking pattern.

7
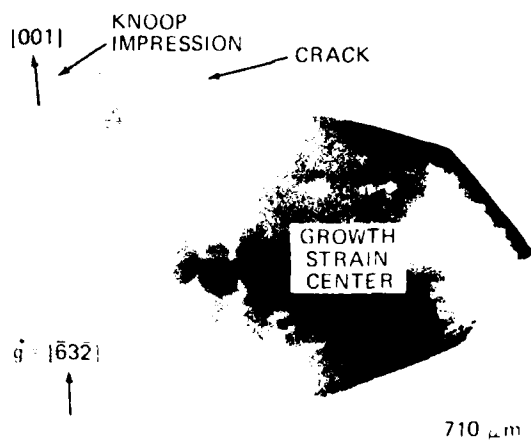
(a) X RAY SURFACE REFLECTION TOPOGRAPH
BEFORE KNOOP HARDNESS MEASUREMENTS
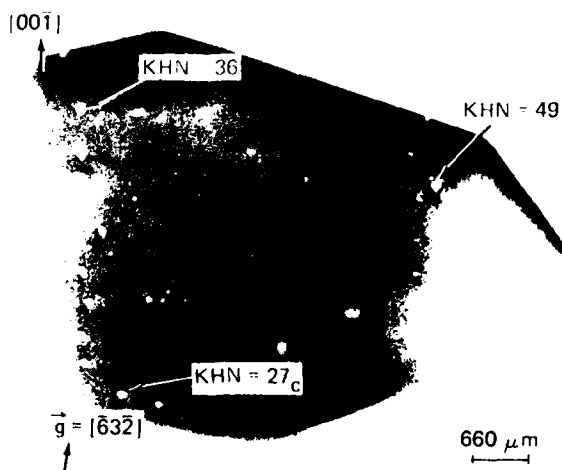
(b) X-RAY SURFACE REFLECTION TOPOGRAPH
AFTER KNOOP HARDNESS MEASUREMENTS

FIGURE 4. BERG-BARRETT TOPOGRAPHS ((6̄32) REFLECTION) BEFORE AND AFTER
KNOOP HARDNESS MEASUREMENTS ON THE (2̄10) GROWTH SURFACE OF
A LABORATORY GROWN RDX CRYSTAL

8

FIGURE 5. STEREOGRAPHIC DESCRIPTION OF X RAY TOPOGRAPHY ALIGNMENT
FOR RDX

9

FIGURE 6. KNOOP HARDNESS ANISOTROPY FOR LABORATORY–GROWN RDX CRYSTAL

(a) LIGHT (ZEISS TESSOVAR) PHOTOGRAPH

(b) REFLECTED LIGHT PHOTOGRAPH

FIGURE 7. VICKERS HARDNESS INDENTATION IN HOLSTEN CLASS D RDX CRYSTAL

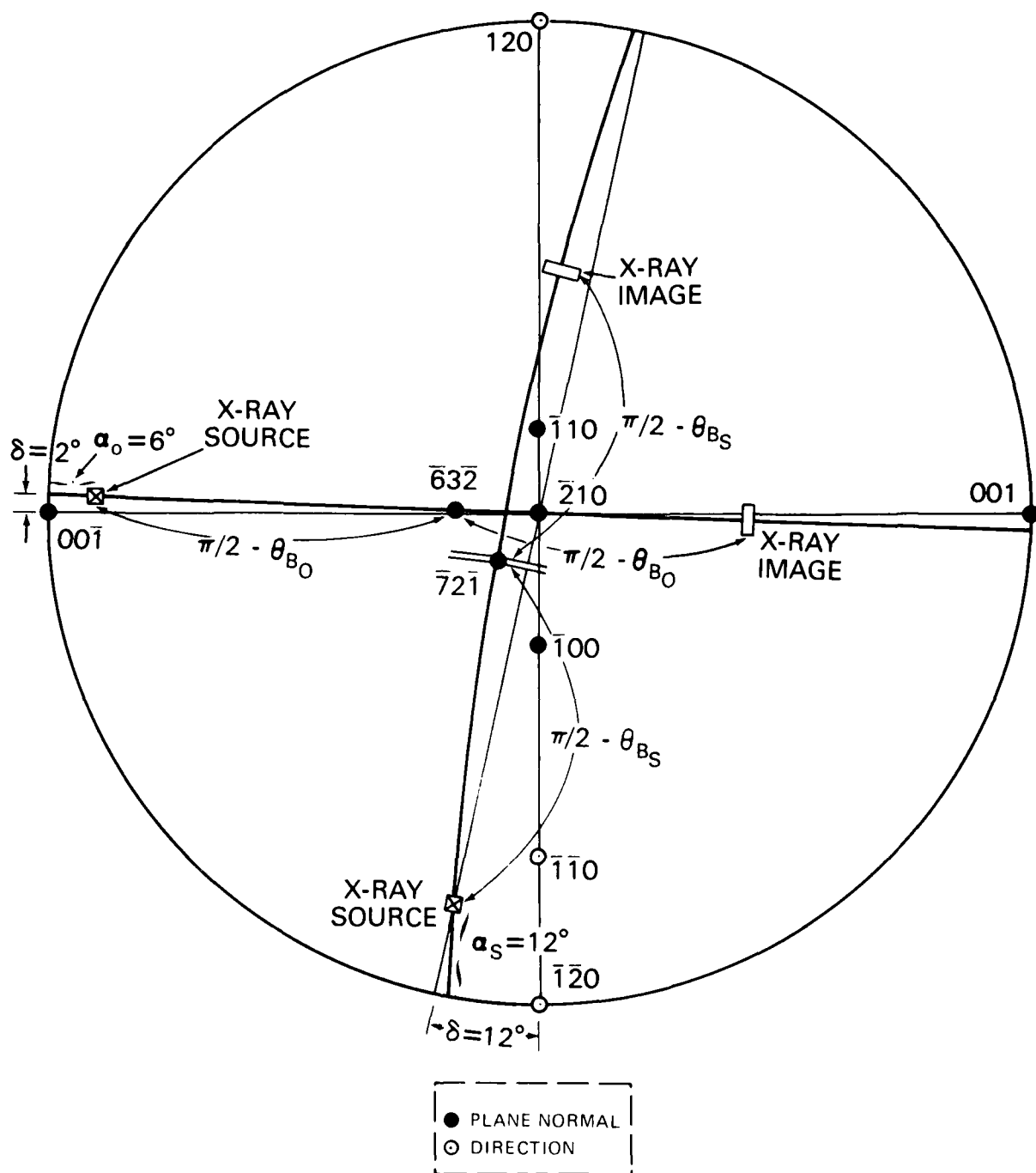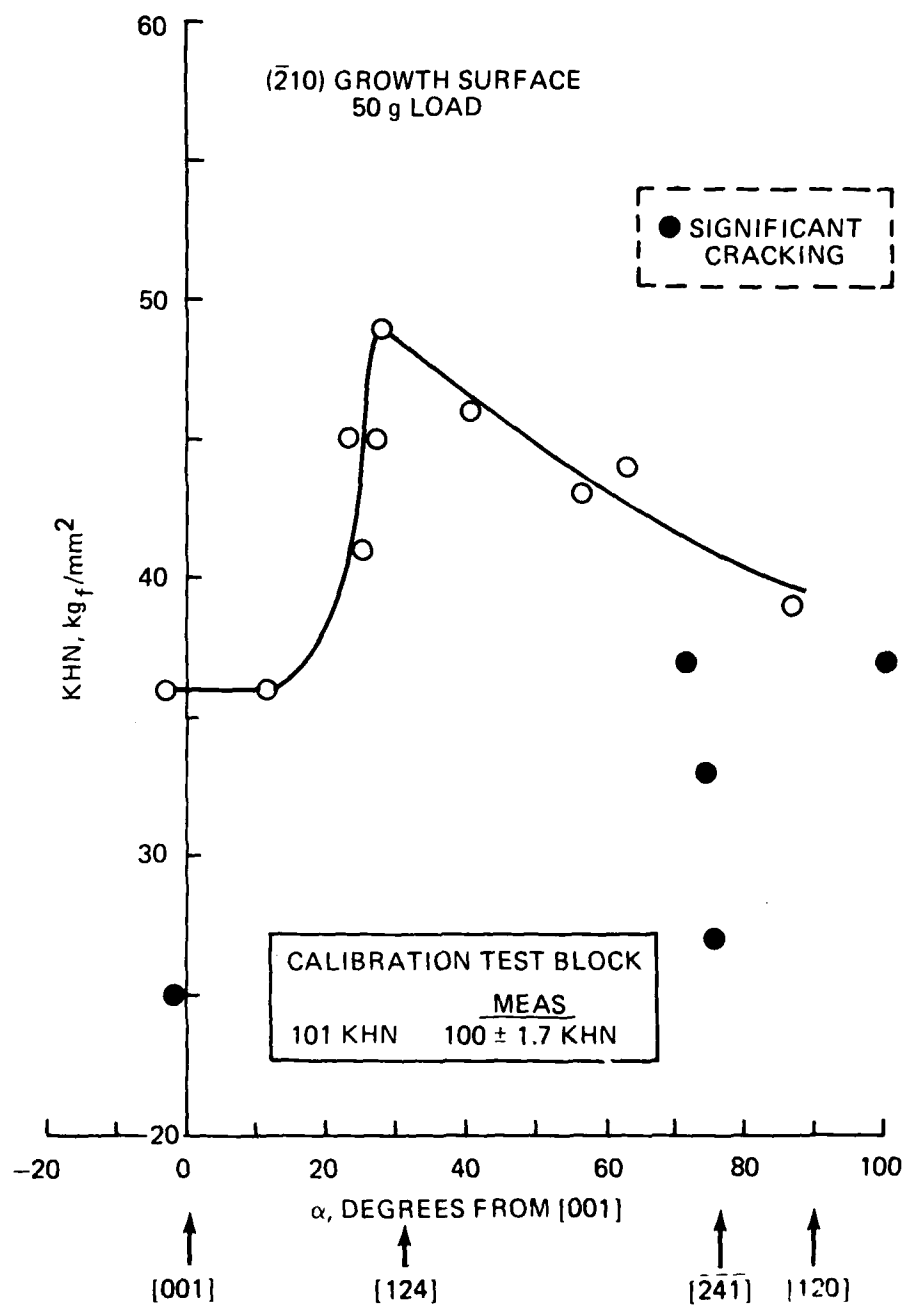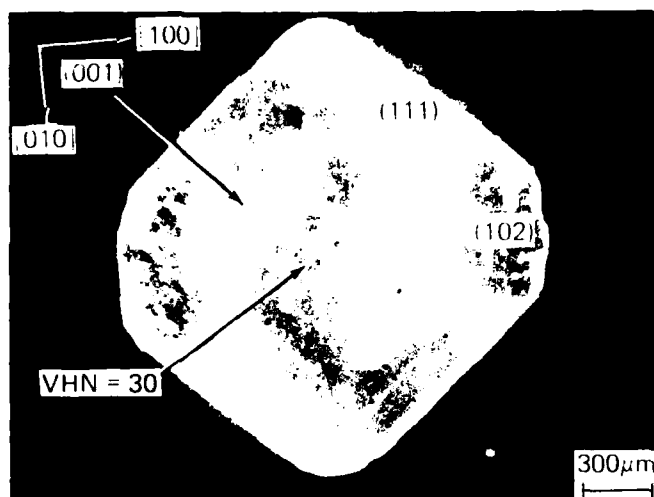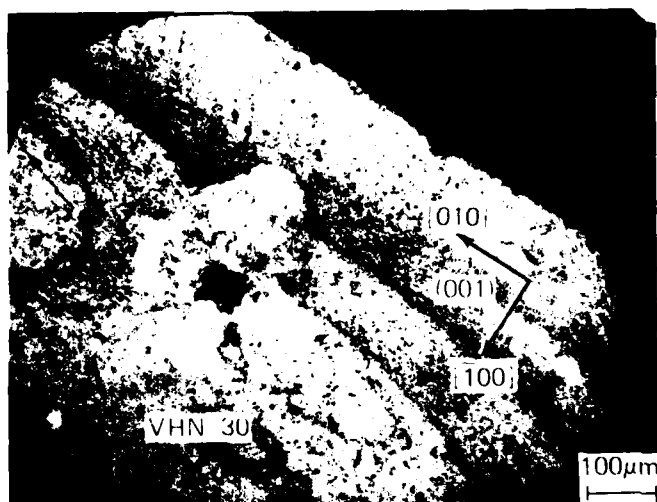Microscopic examination of as-received/indented (Figure 7(a)) and fractured (Figure 8) Holsten Class D crystals revealed the presence of numerous pores. Porosity of this type would explain the large variation in Vickers hardness numbers for these crystals. In addition to performing scanning electron microscopy (SEM) on indentation-induced fracture surfaces of Class D crystals, Dr. M. K. Norr (NSWC, Code R34) examined a number of indentations (e.g., Figure 9) in crystals for evidence of well-defined slip. No surface relief caused by cumulative slip centered on the indentations was observed. However, there was what appeared to be a thin sheared layer that was displaced into the large oblong pore near where the Vickers indentation had been placed into the (001) surface (Figure 8). Interestingly, this sheared layer is curved rather than crystallographic in appearance, suggesting possibly that wavy slip[18] occurred.

FEASIBILITY OF MONITORING CHEMICAL DECOMPOSITION IN FRACTURED RDX CRYSTALS

A brief feasibility study was conducted by Dr. J. C. Hoffsommer (NSWC, Code R16) to assess using various instrumental methods to monitor chemical decomposition in crystalline energetic materials that have been deformed and/or fractured in a controlled manner. Assuming that the amount of gas evolved during the fracture of RDX is the same as that for β-lead azide,[19] it is estimated that a 0.05 g crystal of RDX would experience a 0.00017% weight loss corresponding to 0.0024 mole % decomposition. Thin-layer chromatography, high performance liquid chromatography, and gravimetric methods would all be too insensitive to detect such a small amount of decomposition. However, gas chromatographic analysis (electron capture detector) appears feasible to measure chemical decomposition in fractured RDX crystals, provided an organic (e.g., nitroso) derivative is formed with a retention time sufficiently different from RDX. In the event that RDX is completely degraded to gaseous products, a specially adapted mass spectrometer, such as that described by Fox and Soria-Ruiz,[19] would be needed.

In addition, arrangements were made with Prof. J. T. Dickinson, Washington State University (WSU), to perform fracto-emission experiments at WSU on a number of Holsten production-grade Class D RDX crystals, on a few laboratory-grown RDX crystals that are to be characterized at NSWC, and on various model inert crystals.

EXPERIMENTAL INVESTIGATION OF HOT SPOT FORMATION DURING IMPACT

This work is in support of another effort investigating hot spot formation in crystalline explosives, plastic bonded explosives, and propellants when drop-weight impact loaded. An effort was made to verify theoretical predictions[4,20] that hot spot temperature is proportional to dislocation velocity. Originally, it was planned to use an infrared technique to measure heating as a function of loading rate in samples that were impact loaded. Unfortunately, an equipment problem prevented this. Instead, the time of ignition (based upon measurement of the sample's electrical resistance during impact (with a 5 kg drop weight) was determined as a function of the applied load and the loading rate.

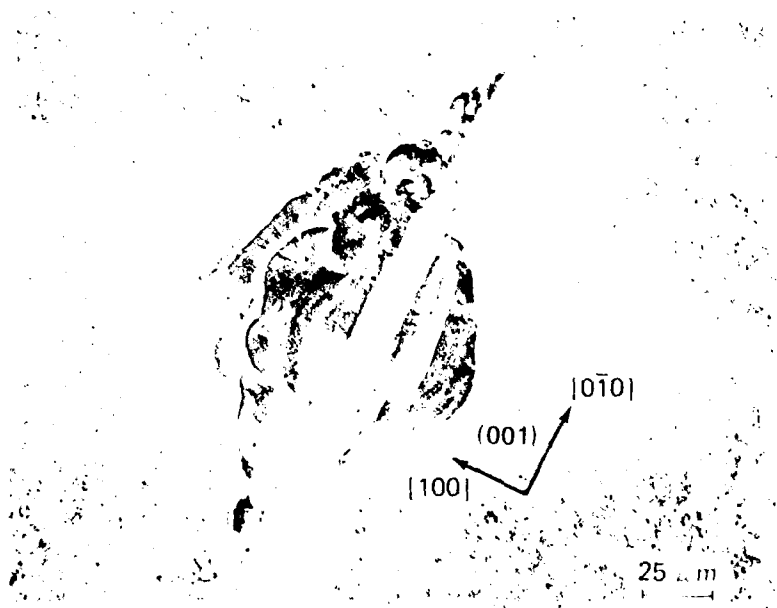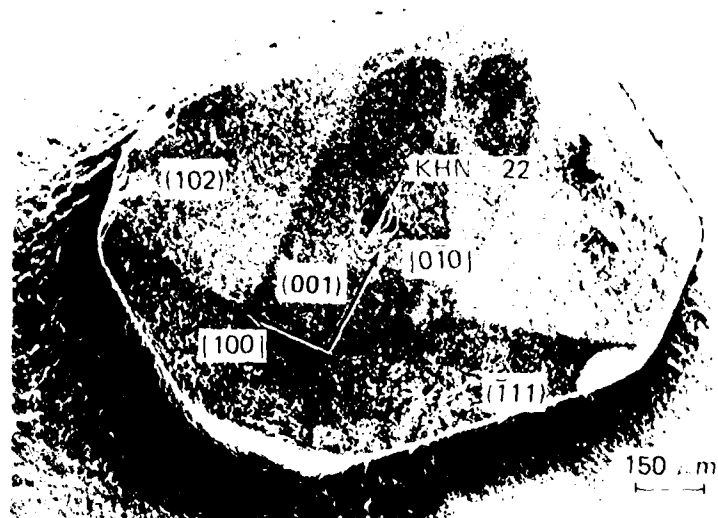FIGURE 8. SEM PHOTOMICROGRAPHS OF FRACTURE SURFACE OF INDENTED HOLSTEN CLASS D RDX CRYSTAL

FIGURE 9 SEM PHOTOMICROGRAPHS OF INDENTED HOLSTEN CLASS D RDX CRYSTAL

A number of neat crystalline and plastic bonded explosives, including RDX, HMX, and PETN (pentaerythritetetranitrate), were studied; the crystalline explosive samples were 30-35 mg pressed discs (5 mm diameter x 1 mm high). For a given threshold loading rate, corresponding to the first observation of ignition, it was noted that ignition occurred at or just after the maximum in the applied force-time history, measured by a strain gage mounted on the anvil. As the loading rate was increased, the force level at which ignition occurs was found to decrease. Most of this decrease occurs just beyond threshold. For PETN, which has been studied most extensively, doubling the loading rate reduces the average force on the sample at ignition by about a factor of 5. Although needing additional verification, this average force seems to be approaching a limiting value for progressively higher loading rates. In a directly related way, as the loading rate increases, ignition occurs with decreasing amounts of sample deformation. Still needed are strain measurements that will allow stress level comparisons.

DEFORMATION OF MODEL INERT MATERIALS

The nature of the plastic deformation resulting from performing hardness experiments on selected model inert crystals was investigated at the University of Maryland, College Park, using Berg-Barrett topography. Among the crystals chosen for eventual study are LiF, NaCl, KCl, and MgO, all having the rock salt structure. They span a significant range in deformation behavior for this crystal structure, from being reasonably ductile, as is LiF, to being relatively brittle, as is MgO. Further, these materials have dislocation structures capable of being characterized by X-ray topography.[17] Previous results obtained on LiF crystals have indicated that it should not be prone to hot spot formation because of its ductility, preventing a discontinuous strain gage response.[21] Alternatively, specific dislocation interactions are known to promote cracking in MgO. Thus, it is of interest to determine whether this cracking behavior[22] is associated with a discontinuous stress-strain response, and how this then relates to hot spot formation. Particular emphasis was given to studying MgO during this reporting period. In addition to the work at the University of Maryland, synchrotron X-ray topography was performed[23] on an indented NaCl crystal at the Cornell High Energy Synchrotron Source (CHESS); this particular aspect of the work was done in collaboration with Mr. R. C. Dobbyn and Dr. M. Kuriyama of the National Bureau of Standards.

Hardness experiments using a 1.59 mm (0.0625 in) diameter spherical indenter (1, 3.5, 15, and 100 kg load) were performed on the (001) cleavage surface of a large (several cm) MgO crystal. A Vickers indenter (25 and 100 g load) was then used to probe the strain field caused by the spherical indenter (100 kg load) in an effort to assess strain hardening. The indentations placed at 15 and 100 kg load are shown in Figure 10(a). A Berg-Barrett topograph ($0\bar{2}2$ reflection) of the same area appears in Figure 10(b). The absence of diffracted intensity (white region) centered at either indentation is readily apparent. Immediately surrounding the white region for the indentation placed at 15 kg load is a region of dislocation enhanced diffracted intensity. By comparison, only a minimal region of enhanced intensity exists for the 100 kg load indentation, even though its size might be expected to scale. This surprising lack of enhanced intensity is caused by an absence of residual dislocations that were able to run out to the $\{110\}$ radial crack surfaces (Figure 11).

15
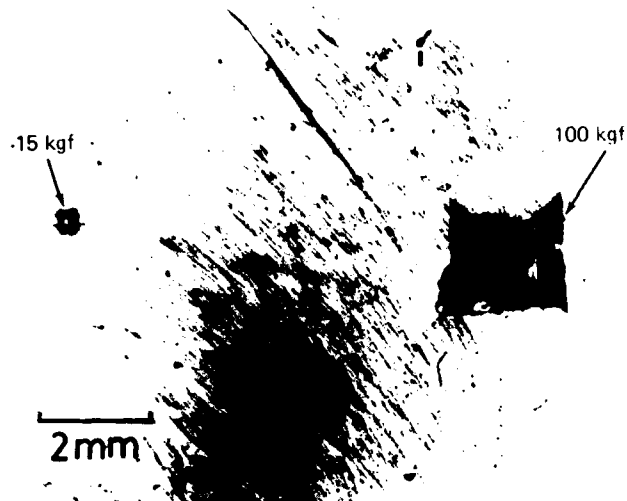
(a) REFLECTED LIGHT PHOTOGRAPH
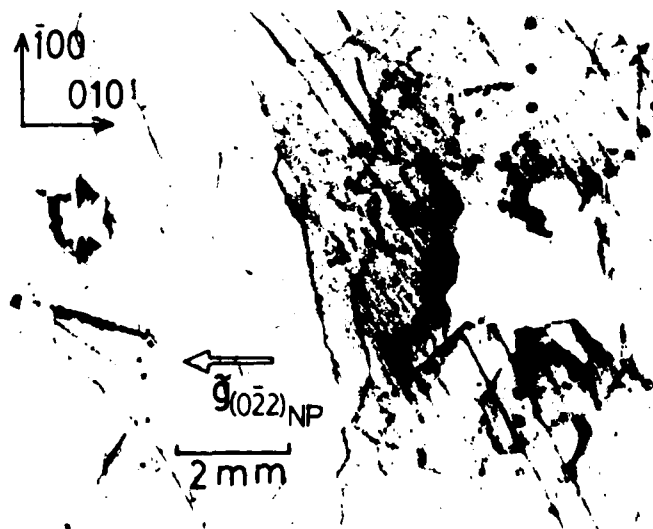
(b) X RAY SURFACE REFLECTION TOPOGRAPH

CuKα RADIATION AT 18 kV AND 20 mA FOR
2 h ON ILFORD L4 50μm NUCLEAR PLATE

FIGURE 10. HARDNESS INDENTATIONS (SPHERICAL INDENTER) IN THE (001)
CLEAVAGE SURFACE OF MgO

2.5 mm

FIGURE 11. ENLARGED VIEW (REFLECTED LIGHT) OF INDENTATION (SPHERICAL
INDENTER AT 100 kg LOAD) IN (001) CLEAVAGE SURFACE OF MgO

Measurements were made (Figure 12) of indentation size and crack length that resulted for the various loads on the ball and Vickers indenters. Microindentation results obtained by Armstrong and Raghuram[9] and dynamic ball measurements reported by Chaudhri, Wells, and Stephens[24] are included. Results in Figure 12 show that a power law relationship exists between force and diagonal crack length with the exponent equaling 3/2 in agreement with a fracture mechanics analysis of Lawn and Fuller.[25]

An effort was made to quantitatively assess the relationship between the strain field surrounding the hardness impression and the cracking that occurred at the indentation site as a function of indenter load. Measurements of the diagonal $\{110\}$ crack length, d_c, and the diagonal length for enhanced X-ray diffraction (i.e., the extent of the strain field), d_x, were made from Berg-Barrett topographs. For the indentation made with the spherical indenter at 100 kg load, d_x = 3-4 mm, d_c = 4.2 mm, and $d_x \lesssim d_c$. At 15 kg load, d_x = 1.8 mm, d_c = 0.8 mm, and $d_x \approx 2.3\ d_c$. For the Vickers impression made at 0.1 kg load, d_x = 0.18 mm, d_c = 0.05 mm, and d_x = 3.6 d_c. Armstrong and Raghuram[9] obtained for a Vickers impression made at 0.05 kg load (the lowest load for which cracking occurred) d_x = 0.2 mm, d_c = 0.03 mm, and d_x = 6.7 d_c. These results indicate that an inverse relationship exists between the size of the strain field surrounding the hardness impression and the extent of $\{110\}$ cracking for MgO single crystals.

Hardness impressions were also placed into the (001) cleavage surface of a large (2x2x1 cm) NaCl (Harshaw) crystal using a 1.59 mm (0.0625 in) diameter spherical indenter (3, 10, and 15 kg load). Synchrotron radiation topographs were obtained[23,26] at the CHESS using the system depicted in Figure 13. A topograph ((0$\bar{4}$4) reflection) of a region of the (001) surface containing three ball indentations appears in Figure 14. The eight-lobed regions of zero diffraction intensity are caused by slip-induced crystal lattice rotations under the spherical indenter. A stereographic projection description of this appears in Figure 15. Observation of the zero intensity regions centered on the indentations is a function of the angular position of the sample with respect to the incident X-ray beam (Figure 16); this sequence of images was photographed from a video screen (the zero diffraction region now appears black).

OPEN SYMBOL   DIAGONAL INDENTATION LENGTH
CLOSED SYMBOL   DIAGONAL CRACK LENGTH
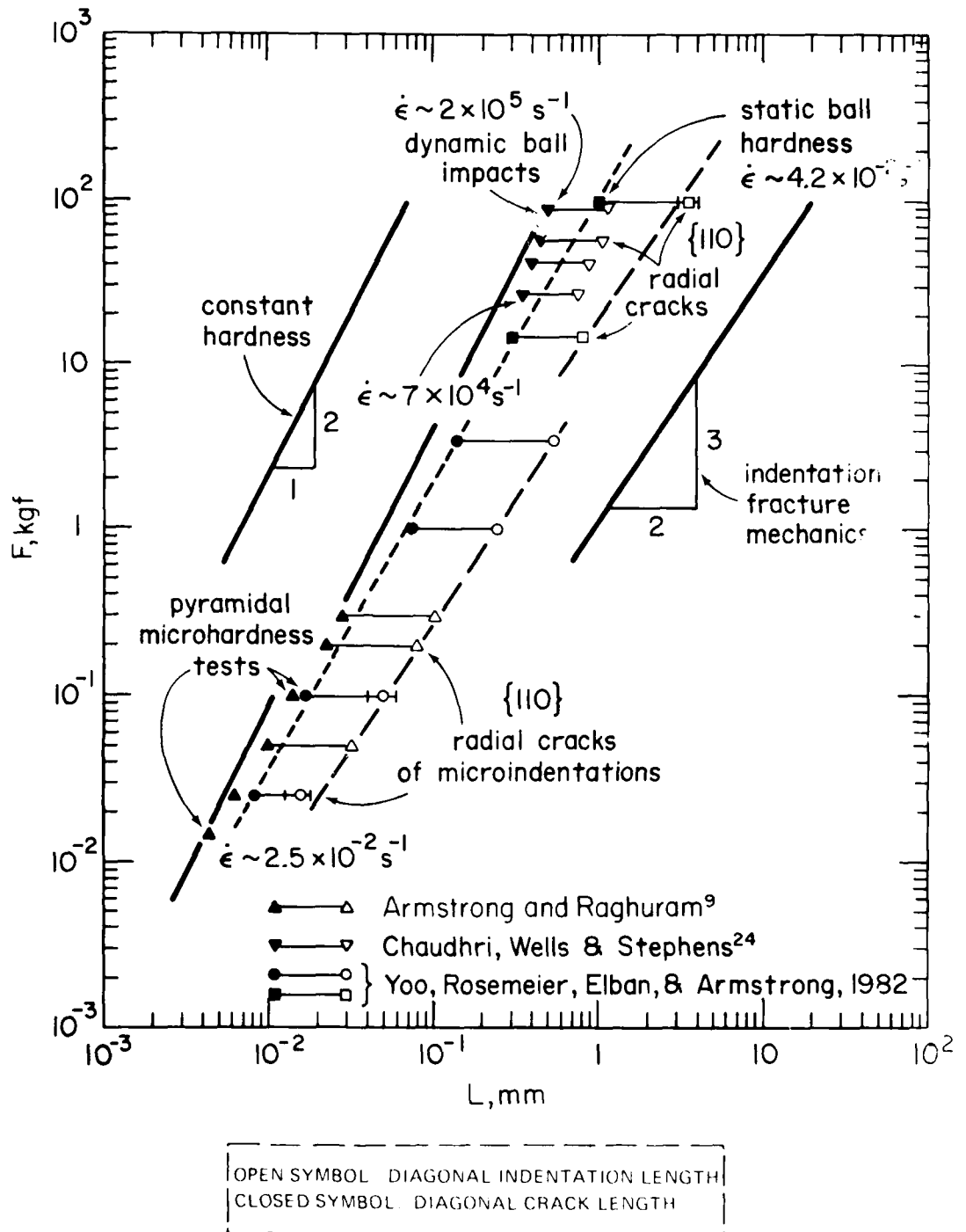
FIGURE-12.   LOGARITHMIC VARIATION OF APPLIED FORCE ON THE INDENTER
VERSUS DIAGONAL INDENTATION AND CRACK LENGTHS FOR MgO
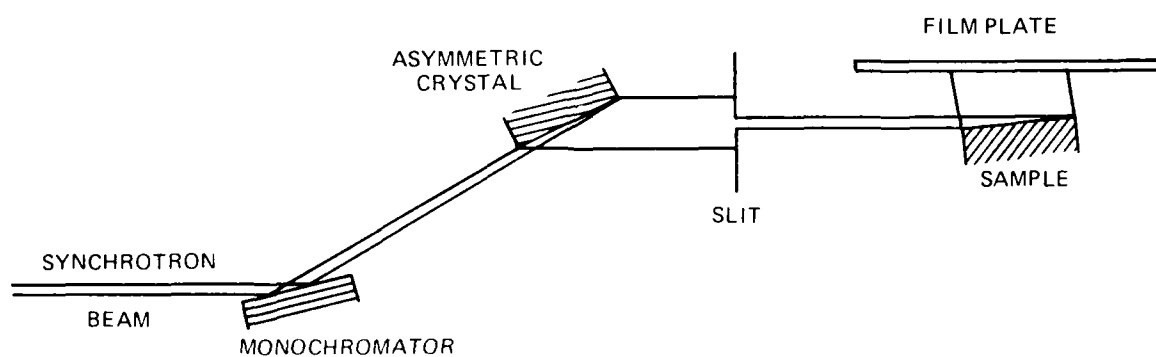
FIGURE 13.   SCHEMATIC OF SYNCHROTRON X-RAY TOPOGRAPHY SYSTEM

(AFTER REFERENCE 23)

[$\bar{1}$00]

[010]

$\vec{g}$ = [0$\bar{4}$4]

0.3 mm

3 kgf

15 kgf

10 kgf
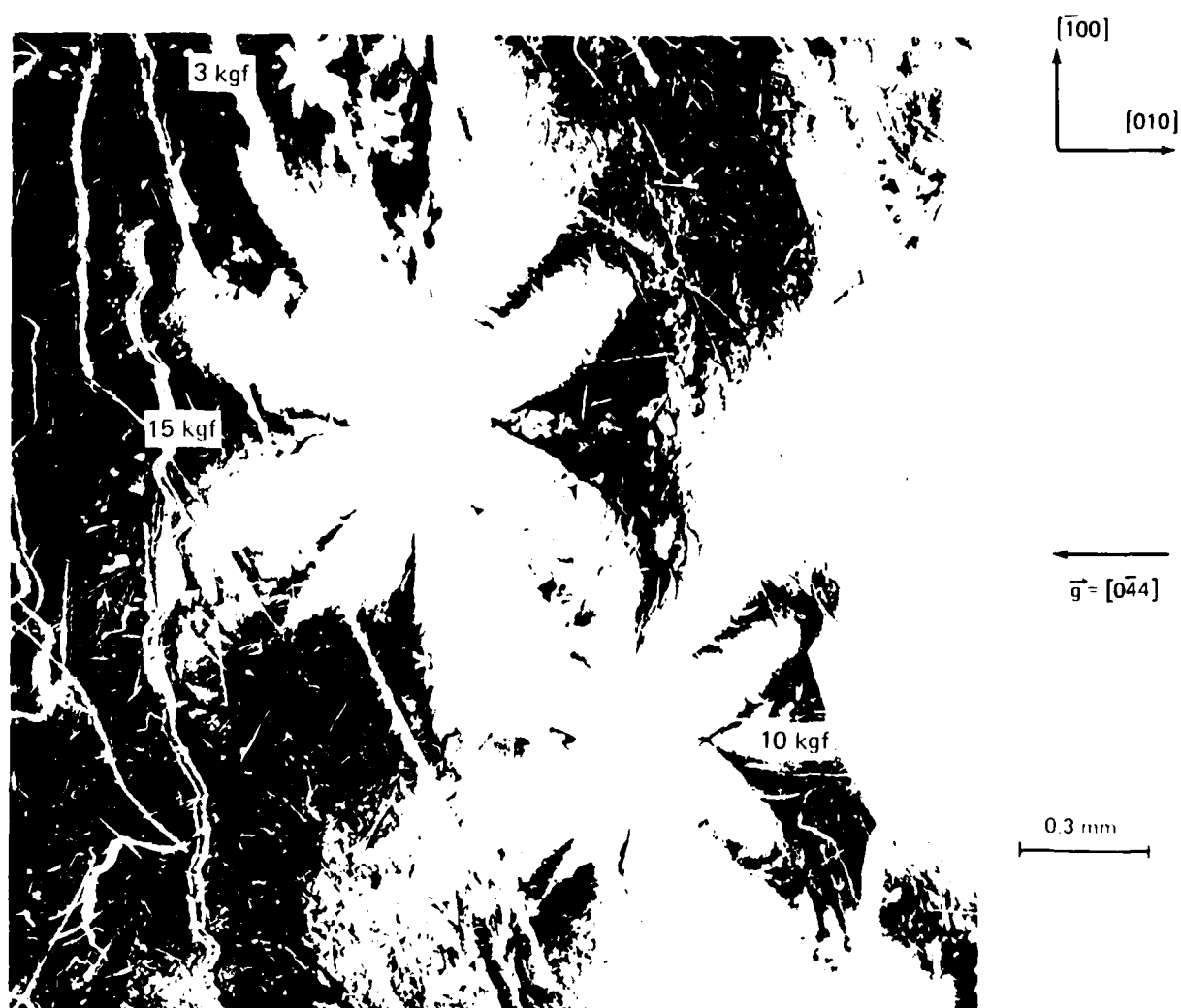
8 keV SYNCHROTRON RADIATION AT 5.25 GeV AND 16 mA
FOR 5 MIN ON ILFORD L4 50 μm NUCLEAR PLATE

FIGURE 14.   SYNCHROTRON X-RAY TOPOGRAPH ((0$\bar{4}$4) REFLECTION) OF INDENTATIONS
(SPHERICAL INDENTER) IN THE (001) CLEAVAGE SURFACE OF NaCl

(AFTER REFERENCES 23 AND 26)

21
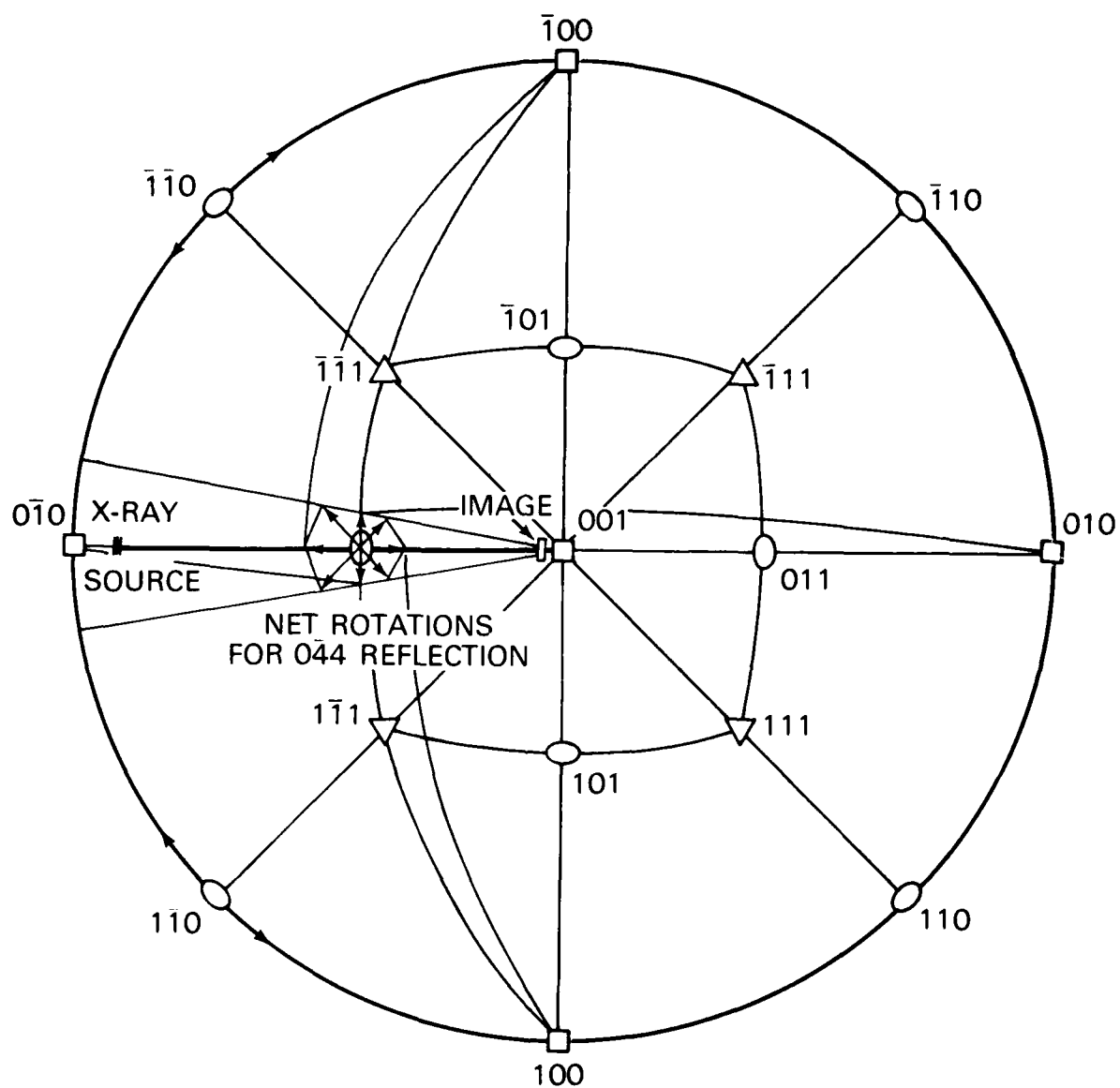
FIGURE 15   STEREOGRAPHIC DESCRIPTION OF X RAY TOPOGRAPHY ALIGNMENT
AND SLIP INDUCED LATTICE ROTATION FOR NaCl

(AFTER REFERENCE 23)
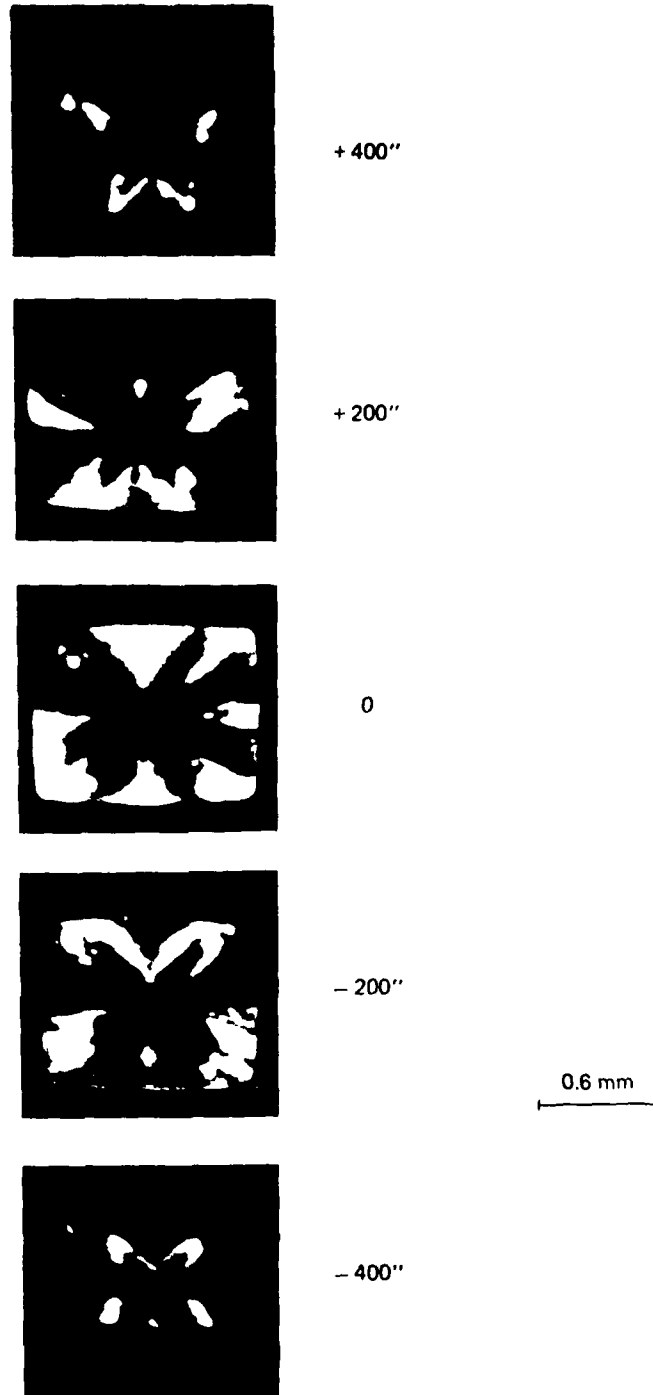
FIGURE 16.   SEQUENCE OF SYNCHROTRON X-RAY TOPOGRAPHS ((0$\bar{4}$4) REFLECTION)
OF INDENTATION (SPHERICAL INDENTER) IN THE (001) CLEAVAGE
SURFACE OF NaCl AS A FUNCTION OF ANGULAR POSITION OF CRYSTAL

(AFTER REFERENCE 23)

23

SUMMARY

Berg-Barrett X-ray topography has been used to characterize growth
perfection and the extent of deformational zones associated with induced
imperfections (i.e., hardness impressions) in a laboratory-grown RDX crystal
having reasonable microstructural perfection. Large, localized internal
stress concentrations are predicted to occur in RDX, helping to explain its
propensity for hot spot formation under drop-weight impact conditions. The
considerable variation in Vickers hardness observed for Holsten production-
grade Class D RDX crystals was attributed to porosity.

A companion study involving hardness experiments and Berg-Barrett
topography (to assess the strain fields surrounding the hardness impressions)
was performed on MgO. This material was selected as a model inert that should
exhibit a discontinuous stress-strain response. It was observed, for applied
loads increasing from 1 to 100 kgf, that the size of the strain fields centered
on the impressions was controlled by cracking. In particular, there was a
virtual absence of dislocations around the indentation placed at 100 kg load
because they ran out $\{110\}$ radial crack surfaces; this was confirmed by the
inability to measure any systematic strain hardening by probing the strain field
with a Vickers indenter at low loads.

REFERENCES

1. Bowden, F. P., and Yoffe, A. D., Fast Reactions in Solids (London: Buttersworths Scientific Publications, 1958).

2. Afanas'ev, G. T., and Bobolev, V. K., Initiation of Solid Explosives by Impact (Jerusalem: Israel Program for Scientific Translations, 1971).

3. Winter, R. E., and Field, J. E., "The Role of Localized Plastic Flow in the Impact Initiation of Explosives," Proceedings of the Royal Society of London, Ser. A, Vol. 343, No. 1634, 1975, pp. 399-413.

4. Armstrong, R. W., Coffey, C. S., and Elban, W. L., "Adiabatic Heating at a Dislocation Pile-Up Avalanche," Acta Metallurgica, Vol. 30, No. 12, 1982, pp. 2111-2116.

5. Fuller, K. N. G., Fox, P. G., and Field, J. E., "The Temperature Rise at the Tip of Fast Moving Cracks in Glassy Polymers," Proceedings of the Royal Society of London, Ser. A, Vol. 361, No. 1705, 1978, pp. 245-263.

6. Weichert, R., and Schönert, K., "Heat Generation at the Tip of a Moving Crack," Journal of the Mechanics and Physics of Solids, Vol. 26, No. 3, 1978, pp. 151-161.

7. Coffey, C. S., Elban, W. L., and Jacobs, S. J., "Detection of Local Heating and Reaction Induced by Impact," in Proceedings of the Sixteenth JANNAF Combustion Meeting, Vol. 1, 10-14 Sep 1979, CPIA Publ. 308, pp. 205-219.

8. Westbrook, J. H., and Conrad, H., Eds., The Science of Hardness Testing and Its Research Applications (Metals Park, OH: American Society for Metals, 1973).

9. Armstrong, R. W., and Raghuram, A. C., "Anisotropy of Microhardness in Crystals," in The Science of Hardness Testing and Its Research Applications, Eds.: Westbrook, J. H., and Conrad, H. (Metals Park, OH: American Society for Metals, 1973), pp. 174-186.

10. Elban, W. L., and Armstrong, R. W., "Microhardness Study of RDX to Assess Localized Deformation and Its Role in Hot Spot Formation," in Proceedings Seventh Symposium (International) on Detonation, 16-19 Jun 1981, NSWC MP 82-334, pp. 976-985.

11. Elban, W. L., Armstrong, R. W., and Hoffsommer, J. C., "X-Ray Orientation and Hardness Experiments on RDX Explosive Crystals," to be published in Journal of Materials Science.

12. Connick, W., and May, F. G. J., "Dislocation Etching of Cyclotrimethylene Trinitramine Crystals," Journal of Crystal Growth, Vol. 5, No. 1, 1969, pp. 65-69.

REFERENCES (Cont.)

13. Urbański, T., Chemistry and Technology of Explosives, Vol. III, First English Edition (Oxford: Pergamon Press, 1967), pp. 87-98.

14. Armstrong, R. W., "Laboratory Techniques for X-Ray Reflection Topography," in Characterization of Crystal Growth Defects by X-Ray Methods, Eds.: Tanner, B. K., and Bowen, D. K. (New York and London: Plenum Press, 1980), pp. 349-367.

15. Farabaugh, E. N., Parker, H. S., and Armstrong, R. W., "Skew Reflection X-Ray Microscopy of the Vapor-Growth Surface of an Al_2O_3 Single Crystal," Journal of Applied Crystallography, Vol. 6, Part 6, 1973, pp. 482-486.

16. Tanner, B. K., X-Ray Diffraction Topography (Oxford: Pergamon Press, 1976).

17. Armstrong, R. W., and Wu, C. Cm., "X-Ray Diffraction Microscopy," in Microstructural Analysis: Tools and Techniques, Eds.: McCall, J. L., and Mueller, W. M., (New York-London: Plenum Press, 1973), pp. 169-219.

18. Stokes, R. J., "Fracture in Ceramics," in Fundamental Phenomena in the Materials Sciences, Vol. 4, Eds.: Bonis, L. J., Duga, J. J., and Gilman, J. J. (New York: Plenum Press, 1967), pp. 151-175.

19. Fox, P. G., and Soria-Ruiz, J., "Fracture-Induced Thermal Decomposition in Brittle Crystalline Solids," Proceedings of the Royal Society of London, Ser. A, Vol. 317, No. 1528, 1970, pp. 79-90.

20. Coffey, C. S., "Phonon Generation and Energy Localization by Moving Edge Dislocations," Physical Review B, Vol. 24, No. 12, 1981, pp. 6984-6990.

21. Heavens, S. N., and Field, J. E., "The Ignition of a Thin Layer of Explosive by Impact," Proceedings of the Royal Society of London, Ser. A, Vol. 338, No. 1612, pp. 77-93.

22. Armstrong, R. W., and Wu, C. Cm., "Lattice Misorientation and Displaced Volume for Microhardness Indentations in MgO Crystals," Journal of the American Ceramic Society, Vol. 61, Nos. 3-4, 1978, pp. 102-106.

23. Yoo, K.-C., Armstrong, R. W., Dobbyn, R. C., and Kuriyama, M., "An Analysis of Local Deformation in Sodium Chloride by Synchrotron Radiation Topography," to be published.

24. Chaudhri, M. M., Wells, J. K., and Stephens, A., "Dynamic Hardness, Deformation and Fracture of Simple Ionic Crystals at Very High Rates of Strain," Philosophical Magazine, Vol. 43, No. 3, 1981, pp. 643-664.

REFERENCES (Cont.)

25. Lawn, B. R., and Fuller, E. R., "Equilibrium Penny-Like Cracks in Indentation Fracture," Journal of Materials Science, Vol. 10, No. 12, 1975, pp. 2016-2024.

26. Kuriyama, M., and Boettinger, W. J., "Application of Synchrotron Radiation to Materials Science," Materials Research Council (DARPA) Workshop on Nondestructive Microstructural Characterization, 6-7 Jul 1982, pp. 166-187.

PRESENTATIONS AND PUBLICATIONS

1. "Investigation of the Origin of Hot Spots in Deformed Materials,"
   W. L. Elban, Workshop on the Fundamentals of Initiation of Chemical
   Decomposition of Energetic Materials, Chestertown, MD, 4-6 May 1982.

2. "X-Ray Orientation and Hardness Experiments on RDX Explosive Crystals,"
   W. L. Elban, R. W. Armstrong, and J. C. Hoffsommer, to be published in
   Journal of Materials Science.

3. "X-Ray Diffraction Topography of Energetic and Inert Crystals,"
   R. W. Armstrong, Workshop on the Fundamentals of Initiation of Chemical
   Decomposition of Energetic Materials, Chestertown, MD, 4-6 May 1982.

DISTRIBUTION

	Copies		Copies

Assistant Secretary of the Navy
(R,E, and S), Room 5E 731
Attn: Dr. L.V. Schmidt   1
Pentagon
Washington, DC 20350

Commandant of the Marine Corps
Attn: Code RD-1,
      Dr. A.L. Slafkosky,   1
      Scientific Advisor
Washington, DC 20380

Office of Naval Research
Attn: Code 430,
      Dr. Richard Miller   10
Arlington, VA 22217

Office of Naval Research
Attn: Code 260, Mr. David Siegel   1
Arlington, VA 22217

Office of Naval Research
Attn: Dr. R.J. Marcus   1
Western Office
1030 East Green Street
Pasadena, CA 91106

Office of Naval Research
Attn: Dr. Larry Peebles,
      Bldg. 114-D   1
East Central Regional Office
666 Summer Street
Boston, MA 02210

Office of Naval Research
Attn: Dr. Phillip A. Miller,
      Suite 601   1
San Francisco Area Office
One Hallidie Plaza
San Francisco, CA 94102

AFATL - DLDL
Attn: Mr. Otto K. Heiney   1
Elgin AFB, FL 32542

AFRPL
Attn: MKP/MS24, Mr. R. Geisler   1
Edwards AFB, CA 93523

AFRPL
Attn: MKPA, Dr. F. Roberto   1
Edwards AFB, CA 93523

Air Force Office of Scientific
      Research
Attn: Dr. L.H. Caveny   1
Directorate of Aerospace Sciences
Bolling Air Force Base
Washington, DC 20332

Air Force Office of Scientific
      Research
Attn: Dr. Donald L. Ball   1
Directorate of Chemical Sciences
Bolling Air Force Base
Washington, DC 20332

FJSRL/NC
Attn: Dr. John S. Wilkes, Jr.   1
USAF Academy, CO 80840

Aerojet Strategic Propulsion Co.
Attn: Dr. R.L. Lou   1
P.O. Box 15699C
Sacramento, CA 95813

Anal-Syn Lab, Inc.
Attn: Dr. V.J. Keenan   1
P.O. Box 547
Paoli, PA 19301

(1)

DISTRIBUTION (Cont.)

	Copies		Copies

Army Ballistic Research Labs
Attn: Code DRDAR-BLT,
  Dr. Philip Howe ... 1
ARRADCOM
Aberdeen Proving Ground, MD 21005

Army Ballistic Research Labs
Attn: Code DRDAR-BLI,
  Mr. L.A. Watermeier ... 1
ARRADCOM
Aberdeen Proving Ground, MD 21005

Commander
U.S. Army Missile Command
Attn: DRSMI-RKL,
  Dr. W. W. Wharton ... 1
Redstone Arsenal, AL 35898

Commander
Army Missile Command
Attn: DRSMI-R, Dr. R.G. Rhoades ... 1
Redstone Arsenal, AL 35898

Atlantic Research Corp.
Attn: Dr. W.D. Stephens ... 1
Pine Ridge Plant
7511 Wellington Rd.
Gainesville, VA 22065

Ballistic Research Laboratory
ARRADCOM
Attn: DRDAR-BLP, Dr. A.W. Barrows ... 1
Aberdeen Proving Ground, MD 21005

Chemical Systems Division
Attn: Dr. C.M. Frey ... 1
P.O. Box 358
Sunnyvale, CA 94086

Cornell University
Attn: Professor F. Rodriguez ... 1
School of Chemical Engineering
Olin Hall, Ithaca, NY 14853

Defense Technical Information
  Center
DTIC-DDA-2
Cameron Station
Alexandria, VA 22314 ... 12

Hercules Incorporated
Attn: Dr. Rocco C. Musso ... 1
Hercules Aerospace Division
Alleghany Ballistic Lab
P.O. Box 210
Washington, DC 21502

Hercules, Inc. Eglin
Attn: Dr. Ronald L. Simmons ... 1
AFATL/DLDL
Eglin AFB, FL 32542

Hercules, Inc.
Attn: Dr. E.H. Debutts ... 1
Baccus Works
P.O. Box 98
Magna, UT 84044

Hercules, Inc. Magna
Attn: Dr. James H. Thacher ... 1
Baccus Works
P.O. Box 98
Magna, UT 84004

Johns Hopkins University APL
Attn: Mr. Theodore M. Gilliland ... 1
Chemical Propulsion Info. Agency
Johns Hopkins Road
Laurel, MD 20810

Lawrence Livermore Laboratory
University of California
Attn: Dr. R. McGuire, Code L-324 ... 1
Livermore, CA 94550

Lockheed Missiles & Space Co.
Attn: Dr. Jack Linsk, Code Org.
  83-10, Bldg. 154 ... 1
P. O. Box 504
Sunnyvale, CA 94088

Armament Development and Test
  Center
Attn: Dr. B.G. Craig ... 1
Eglin Air Force Base, FL 32542

DISTRIBUTION (Cont.)

Copies | Copies

Los Alamos National Lab
Attn: Dr. R.L. Rabie, WX-2,
    MS-952   1
P.O. Box 1663
Los Alamos, NM 87545

Los Alamos Scientific Lab
Attn: Dr. R. Rogers, WX-2   1
P.O. Box 1663
Los Alamos, NM 87545

Naval Air Systems Command
Attn: Code 330, Mr. R. Brown   1
Washington, DC 20360

Naval Air Systems Command
Attn: Dr. H. Rosenwasser,
    AIR-310C   1
Washington, DC 20360

Naval Air Systems Command
Attn: Code 03P25,
    Mr. B. Sobers   1
Washington, DC 20360

Naval Weapons Station
Attn: Dr. L.R. Rothstein,   1
    Assistant Director
Naval Explosives Dev.
Engineering Dept.
Yorktown, VA 23691

Naval Explosives Ordnance
Disposal Tech. Center
Attn: Code D, Dr. Lionel Dickinson   1
Indian Head, MD 20640

Naval Ordance Station
Attn: Code PM4, Mr. C.L. Adams   1
Indian Head, MD 20640

Naval Ordance Station
Attn: Mr. S. Mitchell,
    Code 5253   1
Indian Head, MD 20640

Dean of Research
Attn: Dr. William Tolles   1
Naval Postgraduate School
Monterey, CA 93940

Naval Research Lab
Attn: Code 6100   1
Washington, DC 20375

Naval Research Lab
Attn: Code 6510, Dr. J. Schnur   1
Washington, DC 20375

Naval Sea Systems Command
Attn: Mr. R. Beauregard,   1
    SEA-64E
Washington, DC 20362

Naval Sea Systems Command
Attn: Mr. G. Edwards, SEA-62R3   1
Washington, DC 20362

Naval Ship Engineering Center
Attn: Mr. John Boyle,   1
Materials Branch
Philadelphia, PA 19112

Naval Sea Systems Command
Attn: Mr. J. Murrin, SEA-62R2   1
Washington, DC 20362

Naval Weapons Center
Attn: Code 388, Dr. D.R. Derr   1
China Lake, CA 93555

Naval Weapons Center
Attn: Code 3205,
    Mr. Lee N. Gilbert   1
China Lake, CA 93555

Naval Weapons Center
Attn: Code 3858, Dr. E. Martin   1
China Lake, CA 93555

Copies | Copies

Naval Weapons Center
Attn: Code 3272, Mr. R. McCarten   1
China Lake, CA 93555

Naval Weapons Center
Attn: Code 385, Dr. A. Nielsen   1
China Lake, CA 93555

Naval Weapons Center
Attn: Code 388, Dr. R. Reed, Jr.   1
China Lake, CA 93555

Naval Weapons Center
Attn: Code 3205, Dr. L. Smith   1
China Lake, CA 93555

Naval Weapons Support Center
Attn: Code 5042, Dr. B. Douda   1
Crane, IN 47522

Chief of Naval Technology
Attn: MAT-0716, Dr. A. Faulstich   1
Washington, DC 20360

Chief of Naval Material
Office of Naval Technology
Attn: MAT-0712, LCDR J. Walker   1
Washington, DC 20360

Naval Ocean Systems Center
Attn: Mr. Joe McCartney   1
San Diego, CA 92152

Naval Ocean Systems Center
Attn: Dr. S. Yamamoto   1
Marine Sciences Division
San Diego, CA 91232

Naval Ship Research &
  Development Center
Attn: Dr. G. Bosmajian   1
Applied Chemistry Division
Annapolis, MD 21401

Rohn and Haas Company
Attn: Dr. H. Shuey   1
Huntsville, AL 35801

Strategic Systems Project Office
Department of the Navy
Attn: Dr. J.F. Kincaid, Room 901   1
Washington, DC 20376

Strategic Systems Project Office
Attn: Propulsion Unit,
       Code SP2731   1
Department of the Navy
Washington, DC 20376

Strategic Systems Project Office
Department of the Navy
Attn: Mr. E.L. Throckmorton,   1
       Room 1048
Washington, DC 20376

Thiokol Corporation
Attn: Dr. D.A. Flanigan   1
Huntsville Division
Huntsville, AL 35807

Thiokol Corporation
Attn: Mr. G.F. Mangum   1
Huntsville Division
Huntsville, AL 35807

Thiokol Corporation
Attn: Mr. E.S. Sutton   1
Elkton Division
P.O. Box 241
Elkton, MD 21921

Thiokol Corporation
Attn: Dr. G. Thompson
Wasatch Division   1
MS 240, P.O. Box 524
Brigham City, UT 84302

Thiokol Corporation
Attn: Dr. T.F. Davidson
Government Systems Group   1
P.O. Box 9258
Ogden, UT 84409

Thiokol Elkton Division
Attn: Dr. C.W. Vriesen   1
P.O. Box 241
Elkton, MD 21921

DISTRIBUTION (Cont.)

	Copies		Copies
Thiokol Wasatch Division Attn: Dr. J.C. Hinshaw P.O. Box 524 Brigham City, UT 83402	1	University of California Attn: Professor M.D. Nicol Dept. of Chemistry 405 Hilgard Avenue Los Angeles, CA 90024	1
U.S. Army Research Office Chemical & Biological Sciences Division P.O. Box 12211 Research Triangle Park NC 27709	1	University of California Attn: Professor A.G. Evans Berkeley, CA 94720	1
USA ARRADCOM Attn: Dr. R.F. Walker, DRDAR-LCE Dover, NJ 07801	1	Catholic Univ. of America Attn: Professor T. Litovitz Physics Department 520 Michigan Ave., NE Washington, DC 20017	1
Propellants and Explosives Defense Equipment Staff Attn: Dr. T. Sinden, Munitions Directorate British Embassy 3100 Massachusetts Ave. Washington, DC 20008	1	Graduate Aeronautical Lab Attn: Professor W.G. Knauss California Institute of Tech. Pasadena, CA 91125	1
AFROL/LK Attn: LTC B. Loving Edwards AFB, CA 93523	1	Georgia Institute of Tech. Attn: Professor Edward Price School of Aerospace Engin. Atlanta, GA 30332	1
Institute of Polymer Science Attn: Professor Alan N. Gent University of Akron Akron, OH 44325	1	Hercules Aerospace Division Attn: Dr. Kenneth O. Hartman Hercules Incorporated P.O. Box 210 Cumberland, MD 21502	1
Army Ballistic Research Labs ARRADCOM Attn: DRDAR-BLI, Mr. J. M. Frankle Aberdeen Proving Ground, MD 21005	1	IBM Research Lab Attn: Dr. Thor L. Smith, D42-282 San Jose, CA 95193	1
Army Ballistic Research Labs Attn: Dr. Ingo W. May, DRDAR-BLI ARRADCOM Aberdeen Proving Ground, MD 21005	1	Lockheed Missile & Space Co. Attn: Dr. J.P. Marshall Dept. 52-35, Bldg. 204/2 3251 Hanover Street Palo Alto, CA 94304	1
California Institute of Tech. Attn: Professor N.W. Tschoegl Dept. of Chemical Engineering Pasadena, CA 91125	1	Los Alamos National Lab Attn: Ms. Joan L. Janney, Mail Stop 920 Los Alamos, NM 87545	1

DISTRIBUTION (Cont.)

	Copies		Copies
Los Alamos Scientific Lab Attn: Dr. J.M. Walsh Los Alamos, NM 87545	1	Univ. of Utah Attn: Dr. Stephen Swanson Dept. of Mech. & Industrial Engineering MEB 3008 Salt Lake City, UT 84112	1
Naval Postgraduate School Attn: Prof. Richard A. Reinhardt Physics & Chemistry Dept. Monterey, CA 93940	1	Thiokol Corporation Attn: Mr. J.D. Byrd Huntsville Division Huntsville, AL 35807	1
Northwestern University Attn: Professor J.D. Achenbach Dept. of Civil Engineering Evanston, IL 60201	1	Washington State University Attn: Professor G.D. Duvall Dept. of Physics Pullman, WA 99163	1
Office of Naval Research Attn: Dr. N.L. Basdekas Mechanics Program, Code 432 Arlington, VA 22217	1	Washington State University Attn: Prof. T. Dickinson Dept. of Physics Pullman, WA 99163	1
Pennsylvania State Univ. Attn: Professor Kenneth Kuo Dept. of Mechanical Engineering University Park, PA 16802	1	Department of the Navy Office of Naval Research Attn: Dr. R.W. Armstrong Branch Office, Box 39 FPO, New York 09510	5
Sandia Laboratories Attn: Dr. S. Sheffield, Division 2513 P.O. Box 5800 Albuquerque, NM 87185	1	Naval Sea Systems Command Attn: SEA-06R, Dr. D.J. Pastine Washington, DC 20362	1
Space Sciences, Inc. Attn: Dr. M. Farber 135 Maple Avenue Monrovia, CA 91016	1	Office of Naval Research Attn: MAT-0727, Dr. E. Zimet Arlington, VA 22217	1
Washington State University Attn: Prof. Y. M. Gupta Dept. of Physics Pullman, WA 99163	1	Wasington State University Attn: Prof. M. Howard Miles Dept. of Physics Pullman, WA 99163	1
SRI International Attn: Mr. M. Hill 333 Ravenswood Avenue Menlo Park, CA 94025	1	University of Maryland Attn: Dr. K.-C. Yoo Department of Mechanical Engineering College Park, MD 20742	10
Texas A&M Univ. Attn: Prof. Richard A. Schapery Dept. of Civil Engineering College Station, TX 77843	1		

DISTRIBUTION (Cont.)

	Copies		Copies
University of Maryland		Internal Distribution (Cont.):	
Attn: Dr. R. G. Rosemeier	10	R12 (Elzufon)	1
Department of Mechanical		R12 (Bowen)	1
Engineering		R121 (Stosz)	1
College Park, MD 20742		R122 (Roslund)	1
		R13 (Dickinson)	1
National Bureau of Standards		R13 (Bernecker)	1
Attn: Dr. Masao Kuriyama	2	R13 (Chiarito)	1
Bldg. 223, Room B266		R13 (Clairmont)	1
Washington, DC 20234		R13 (Coffey)	5
		R13 (Coleburn)	1
Naval Weapons Center		R13 (DeVost)	1
Attn: Code 3858, Dr. Rena Y. Yee	1	R13 (Elban)	25
China Lake, CA 93555		R13 (Forbes)	1
		R13 (Jacobs)	1
Naval Weapons Center		R13 (Jones)	1
Attn: Code 3882, Mr. Thomas Boggs	1	R13 (Kim)	1
China Lake, CA 93555		R13 (Price)	1
		R13 (Sandusky)	1
Internal Distribution:		R14 (Marshall)	1
R (Wessel)	1	R15 (Pittman)	1
R10 (Proctor)	1	R16 (Haiss)	1
R11 (Mueller)	1	R16 (Hoffsommer)	1
R11 (Adolf)	1	R34 (Norr)	1
R11 (Holden)	1	E35	1
R11 (Kamlet)	1	E431	9
		E432	3

END

DATE
FILMED

9 – 83

DTIC